Toward Active Control of Noise
from Hot Supersonic Jets

Quarterly Progress Report No. 9

1 October 2013 – 31 December 2013

Nathan E. Murray (PI)
National Center for Physical Acoustics
The University of Mississippi
University, MS 38677
(662) 915-3190
nmurray@olemiss.edu

Charles E. Tinney (Co-PI) – The University of Texas at Austin
Praveen Panickar – Combustion Research and Flow Technology, Inc.

Contract: N00014-11-1-0752

Attn: Joseph Doychak & Brenda Henderson
Office of Naval Research
Arlington, VA 22203-1995
joseph_doychak@onr.mil | brenda.s.henderson@navy.mil

Executive Summary

Experimental measurements of a cold, shock-free, Mach 3.0 jet were completed. Current analyses suggest a transition in the near-field between cylindrical and spherical spreading. The results also suggest cumulative non-linear distortion can be detected in the near-field. Comparison with previous measurements suggest that the ambient conditions (relative humidity) during the experiment play a vital role in reproducing non-linear propagation effects. Other work completed during this reporting period includes the generation of a computational data set for analysis of the waveform propagation under WBS 1.1.

20151013115

December 31, 2013

REPORT DOCUMENTATION PAGE

1. REPORT DATE *(DD-MM-YYYY)*	2. REPORT TYPE		3. DATES COVERED *(From - To)*
12/31/2013	Interim Research Performance Report		10/1/2013 - 12/31/2013

4. TITLE AND SUBTITLE	5a. CONTRACT NUMBER
Interim Research Performance Report Quarterly Report No. 9	
	5b. GRANT NUMBER
	N00014-11-1-0752
	5c. PROGRAM ELEMENT NUMBER

6. AUTHOR(S)	5d. PROJECT NUMBER
Nathan E. Murray, Charles E. Tinney (U. of Texas at Austin), Praveen Panickar (CRAFT Tech.)	
	5e. TASK NUMBER
	5f. WORK UNIT NUMBER

7. PERFORMING ORGANIZATION NAME(S) AND ADDRESS(ES)	8. PERFORMING ORGANIZATION REPORT NUMBER
The University of Mississippi Jamie Whitten National Center for Physical Acoustics University, MS 38677	

9. SPONSORING/MONITORING AGENCY NAME(S) AND ADDRESS(ES)	10. SPONSOR/MONITOR'S ACRONYM(S)
Joseph Doychak Office of Naval Research 875 North Randolph Street Arlington, VA 22203-1995	ONR
	11. SPONSOR/MONITOR'S REPORT NUMBER(S)

12. DISTRIBUTION/AVAILABILITY STATEMENT

Approved for Public Release; Distribution is Unlimited

13. SUPPLEMENTARY NOTES

14. ABSTRACT

Experimental measurements of a cold, shock-free, Mach 3.0 jet were completed. Current analyses suggest a transition in the near-field between cylindrical and spherical spreading. The results also suggest cumulative non-linear distortion can be detected in the near-field. Comparison with previous measurements suggest that the ambient conditions (relative humidity) during the experiment play a vital role in reproducing non-linear propagation effects. Other work completed during this reporting period includes the generation of a computational data set for analysis of the waveform propagation under WBS 1.1.

15. SUBJECT TERMS

Jet Noise Reduction, High Dynamic Range PIV, Computational Phased Array Beamforming, Aeroacoustics

16. SECURITY CLASSIFICATION OF:			17. LIMITATION OF ABSTRACT	18. NUMBER OF PAGES	19a. NAME OF RESPONSIBLE PERSON
a. REPORT	b. ABSTRACT	c. THIS PAGE			Nathan E. Murray
				28	**19b. TELEPHONE NUMBER** *(Include area code)* 662-915-3190

Contents

1 Project Objectives and Status

1.1 Review of Program Objectives

Our current objectives are focused on the propagation of noise generated by supersonic jets.

1. Determine whether shock-like structures are emitted as such from the jet or if they are the result of rapid steepening immediately outside of the jet.
2. Determine the appropriate decay law for the acoustic field.

1.2 Project Status

This reporting period marks the first quarter of effort on the grant extension. The extension was formally awarded on 23 October 2013 with the period of performance extended through 30 September 2014 by a subsequent modification. Figure 1 shows the project status. The following list summarizes progress on specific WBS entries.

WBS 1.1 Computational data was generated for analysis of the waveforms by running additional iterations of the LES simulation created during the base effort. Snapshots were saved at 200 kHz sample rate with a much larger spatial domain than that in the base effort. Details are given in Section 2.1.

WBS 1.2 Acoustic measurements for a shock-free, cold, Mach 3.0 jet were completed at UT Austin. Measurement detail and current results were submitted as an abstract to the 2014 AIAA Aeroacoustics Conference. The abstract is attached as Appendix A. Highlights of the results to date are discussed in Section 2.2.

WBS	Task	Start	End	% Complete	2013 Q4	2014 Q1	Q2	Q3	Q4
	N00014-11-1-0752 Extension Work Plan	10/1/13	12/30/14	20					
1	Determine Amplitude and Decay Rate of Acoustic Waveform	10/1/13	9/30/14	22					
1.1	Separating hydrodynamic and acoustic components of the waveform.	10/1/13	3/31/14	25					
1.2	Conduct measurements on a Mach 3 shock-free jet using 1/8-inch microphones.	10/1/13	12/31/13	100					
1.3	Develop Gol'dburg numbers for jet noise problems.	1/1/14	6/30/14	0					
1.4	Demonstrate and validate the decay law findings with acoustic data from hot, shock-containing jets.	4/1/14	9/30/14	0					
2	Prepare Quarterly Reports	1/15/14	10/15/14	25					
2.1	Q-01 Report	1/15/14	1/15/14	100					
2.2	Q-02 Report	4/15/14	4/15/14	0					
2.3	Q-03 Report	7/15/14	7/15/14	0					
2.4	Q-04 Report	10/15/14	10/15/14	0					
3	Present Results at Annual Review Meetings	7/16/14	7/16/14	0					
4	Prepare Final Report	10/1/14	12/30/14	0					

Figure 1. Project chart showing WBS items and current completion status.

2 Activity for Current Reporting Period

2.1 Generation of Computational Data to Support WBS 1.1

New LES data were generated with a much larger spatial domain than that extracted in the base effort. The LES domain itself is quite large; however, in the base effort a restricted spatial extent was captured for post-processing. A wavenumber/frequency analysis was performed on the data, but the findings were limited due to the small radial spatial domain extracted from the full simulation. To support the Fourier and wavelet analyses in WBS 1.1, the LES was re-run and snapshots were saved at 200 kHz with a spatial domain larger in both radial and axial extent compared to the base effort.

Figure 2 graphically shows a comparison in the spatial extent of the extracted data. The new data (left) covers a spatial domain significantly larger in both the axial and radial directions. This larger domain will allow for the development of the waveforms to be explored in greater detail.

2.2 Measurements of Sound Propagation from a Mach 3.0 Cold Jet

Measurements of the acoustic field generated by a cold, shock-free, Mach 3.0 jet were completed in September 2013. The use of $1/8^{th}$ microphones provided an enhanced resolution compared to the previous measurements. Eight microphones were placed along rays emanating from the post-potential core region at various inclination angles relative to the jet axis.
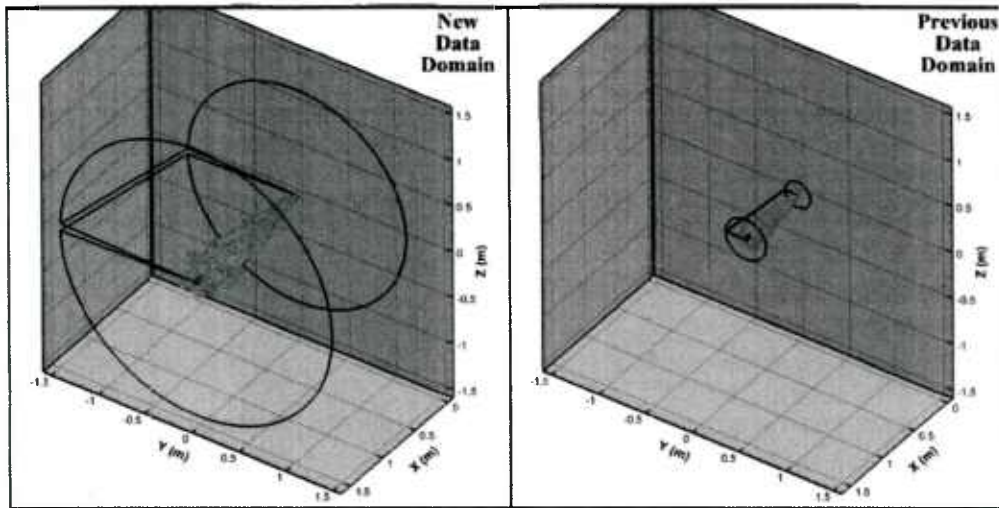
Figure 2. Comparison of the spatial domain extracted from the LES for the WBS 1.1 analyses (left) compared to the smaller domain extracted for analyses under the base effort (right).

Details of the measurements and preliminary results are included in Appendix A and B. Appendix A is an abstract submitted to the 2014 AIAA Aeroacoustics conference. Appendix B is an electronic copy of the presentation given at the 2013 APS-DFD Conference in Pittsburgh.

The new measurements extend the resolved frequency range and provide measurements closer to the jet than previously acquired. The growth in P_{rms}^{-1} (indicative of decay in P_{rms}) along rays inclined at 45° and 65° both show indications that the acoustic spreading follows a cylindrical decay $(1/\sqrt{\rho})$ very near the jet and transitions to spherical (ρ^{-1}). Along the 65° ray, the transition occurs near $50D_j$ as shown in Figure 3.

Figure 3. Growth in P_{rms}^{-1} along a ray inclined 65° to the jet axis (from Figure 6 in Appendix A).

3 Technical/Cost Status & Problem Areas

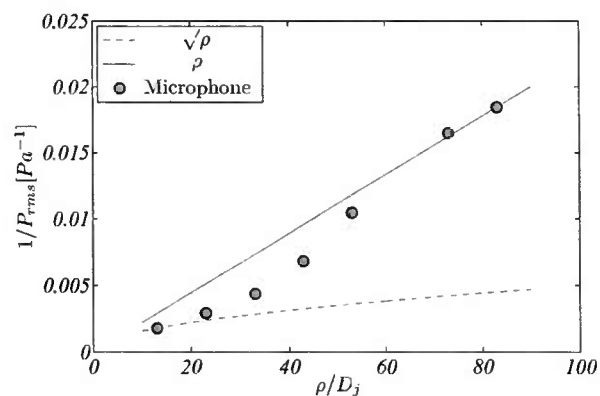All of the subcontracting paperwork has been fully executed to fund collaborators at UT Austin and CRAFT Tech.

4 Publications, Meetings, and/or Travel

- Dr. Tinney's student, Romain Fiévet, presented recent experimental results on the cold Mach 3.0 jet at the 2013 APS-DFD meeting in Pittsburgh. The presentation is included in Appendix B.

- Results from the work performed by Dr. Baars and Dr. Tinney under the base effort were recently published in a book, *Fluid-Structure-Sound Interactions and Control*. The reference is included in the following publication list.

4.1 Running List of Publications Produced

[1] BAARS, W.J., TINNEY, C.E., MURRAY, N.E., JANSEN, B.J. & PANICKAR, P. (2011) "The Effect of Heat on Turbulent Mixing Noise in Supersonic Jets," in *49th AIAA Aerospace Sciences Meeting*, Paper 2011-1029 (Orlando, FL).

[2] BAARS, W.J., TINNEY, C.E. & WOCHNER, M.S. (2012) "Nonlinear Noise Propagation from a Fully Expanded Mach 3 Jet," in *50th AIAA Aerospace Science Meeting*, Paper 2012-1177 (Nashville, TN).

[3] MURRAY, N.E., LYONS, G.W., TINNEY, C.E., DONALD, B., BAARS, W.J., THUROW, B.S., HAYNES, R.H. & PANICKAR, P. (2012) "A Laboratory Framework for Synchronous Near/Far-Field Acoustics and MHz PIV in High-Temperature, Shock-Containing, Jets," in *Proceedings of the Internoise 2012/ASME NCAD Meeting*, ASME/NCAD-1270 [invited] (New York City, NY).

[4] BAARS, W.J. & TINNEY, C.E. (2012) "Scaling Model for Nonlinear Supersonic Jet Noise," in *Bulletin of the American Physical Society*, **57**:17, Abstract D24:8 (San Diego, CA).

[5] PANICKAR, P., ERWIN, J., SINHA, N., MURRAY, N.E. & LYONS, G.W. (2013) "Localization of Acoustic Sources in Shock-Containing Jet Flows Using Phased Array Measurements," in *51st AIAA Aerospace Sciences Meeting*, 2013-0613 (Grapevine, TX).

[6] HAYNES, R.H., BROCK, B.A. & THUROW, B.S. (2013) "Application of MHz Frame Rate, High Dynamic Range PIV to a High-Temperature, Shock-Containing Jet," in *51st AIAA Aerospace Sciences Meeting*, 2013-0774 (Grapevine, TX).

[7] FIÉVET, R., TINNEY, C.E., MURRAY, N.E., LYONS, G.W. & PANICKAR, P. (2013) "Acoustic Source Indicators using LES in a Fully Expanded and Heated Supersonic Jet," in *19th AIAA/CEAS Aeroacoustics Conference*, 2013-2193 (Berlin, Germany).

[8] BAARS, W.J. & TINNEY, C.E. (2013) "Quantifying Crackle-Inducing Acoustic Shock-Structures Emitted by a Fully-Expanded Mach 3 Jet," in *19th AIAA/CEAS Aeroacoustics Conference*, 2013-2081 (Berlin, Germany).

[9] BAARS, W.J. & TINNEY, C.E. (2013) "A Temporal and Spectral Quantification of the Crackle Component in Supersonic Jet Noise," in *2nd Symposium on Fluid-Structure-Sound Interactions and Control*, p. 170 (Shatin, Hong Kong).

[10] BAARS, W.J., TINNEY, C.E. & WOCHNER, M.S. "Nonlinear Distortion of Acoustic Waveforms from High-Speed Jets," *J. of Fluid Mechanics* [in review].

[11] BAARS, W.J. (2013) *Acoustics from High-speed Jets with Crackle*, Ph.D. Dissertation, The University of Texas at Austin.

[12] FIÉVET, R., BAARS, W.J., SILVA, D. & TINNEY, C.E. (2013) "High Fidelity Measurements in the Far-Field of a Mach 3 Jet," in *Bulletin of the American Physical Society*, **58**:18, Abstract D24:7 (Pittsburgh, PA).

[13] BROCK, B.A., HAYNES, R.H., THUROW, B.S., LYONS, G.W. & MURRAY, N.E. (2014) "An Examination of MHz Rate PIV in a Heated Supersonic Jet," in *AIAA Science and Technology Forum and Exposition (SciTech 2014)*, 2014-1102 (National Harbor, MD).

[14] BAARS, W.J. & TINNEY, C.E. (2014) "Temporal and Spectral Quantification of the Crackle Component in Supersonic Jet Noise," in Y. Zhou, Y. Liu, L. Huang & D.H. Hodges, eds., *Fluid-Structure-Sound Interactions and Control*, Lecture Notes in Mechanical Engineering, pp. 205–210 (Springer Berlin Heidelberg).

5   Planned Activities for Next Reporting Period

- Continue analysis of LES data and experimental data under WBS 1.1 and 1.2.
- Prepare for acoustic testing in the NCPA facility under WBS 1.4.

Appendix A: 2014 AIAA/CEAS Aeroacoustics Abstract
Non-linear Acoustic Analysis of a Cold Supersonic Jet
Fiévet, Tinney & Baars

Non-linear acoustic analysis of a cold supersonic jet.

Romain Fiévet[*] and Charles E. Tinney[†]

Aerospace Eng. and Eng. Mechanics, The University of Texas at Austin, Austin, TX 78712, USA

Woutijn J. Baars[‡]

The University of Melbourne, Parkville, Victoria 3010, Australia

The acoustic field of a fully-expanded Mach 3 jet is investigated through an extension of the experiment of Baars & Tinney[1] using higher-fidelity instruments. The previous experiment provided an understanding of non-linearities directivity pattern in the jet near-field, and have also deduced the absence of cumulative distortion. In this new study measurements were acquired along arrays emanating from what appears according to the results of Baars & Tinney as being the main source of sound. The microphones were placed closer to the jet in order to extend the domain of study, enhancing the understanding of the evolution of non-linearities when being closer to the sound source. The main differences between the two experimental campaigns are the following : a resolution of higher frequencies (140kHz against 70kHz for Baars & Tinney), the placement of microphones closer to the jet for the new experiment, and finally a much lower humidity rate for the new one (reducing thereby the atmospheric absorption). The computations of both spectral and scalar indicators of waveform non-linearity such as the Morfey-Howell indicator, the number of zero-crossing or the skewness of the time derivative, seem to support the idea that cumulative non-linear distortion do happen in the near-field at laboratory scale. The spatial derivatives of these metrics indicate a concentration of the activity of wave steepening and shock coalescence (footprints of non-linear distortion) in the close proximity of the jet. Several explanations regarding the apparently contradictory conclusions of the two studies are postulated, based on the main differences in the experimental conditions listed above. Comparisons between raw waveforms acquired either on the far-field or on the near-field seem to confirm the presence of cumulative distortion localized in the vicinity of the source only.

I.   Introduction

Non-linear distortions within an acoustic signal are responsible for the creation of shock-waves, or saw-tooth waves, which are held to be an important source of noise in supersonic jet flows[6,10,14] . Recent studies by Baars & Tinney [2] have provided an understanding of the overall sound pressure topography, identifying the region located after the collapse of the potential core as being the apparent main source of noise radiating to the far-field. It has also shown that despite the presence of crackle no evident trace of presence of cumulative non-linear distortion was found in the region studied and along the peak noise path, under their particular experimental conditions. An experimental campaign consisting in revisiting the experiment of Baars & Tinney [2] in the same anechoic chamber at The University of Texas at Austin using higher fidelity instruments (1/8th inch pressure field microphones resolving up to 140kHz +/-·1dB) is the core of this study. Their previous results are used to define an appropriate spatial placement of the microphones consisting of arrays positioned at key-angles from the jet-centerline originating from the post-potential core region. The goal of this study is to investigate using these new microphones the presence of non-linear distortions over a broader range of frequency on the sound radiated to the far-field by a fully-expanded shock-free supersonic

*PhD Student, AIAA Student Member.

†Assistant Professor, AIAA Senior Member. http://www.ae.utexas.edu/facultysites/tinney/

‡Post-Doctoral Research Fellow, AIAA Member.

jet at laboratory scale. Under these conditions the prominent component of noise is turbulent mixing noise, in the form of Mach waves radiating to the far-field.

The impact of the high humidity rate (HR) under which Baars & Tinney [2] ran their experiment is known to attenuate the strength of non-linear features through absorption,[3] therefore this new experiment was ran at much lower HR allowing a direct comparison of its effect. Additionally, as the previous results enlightened both the absence of cumulative distortion and the presence of non-linearities (i.e. shock waves) in the far-field, it suggests that wave steepening occurs further upstream. In this new experiment arrays of microphones were therefore placed closer to the jet in order to investigate the characteristic of the pressure waveform closer to its source.

The interest of performing the study along arrays is to quantify the importance of cumulative non-linear distortion along the propagation path, as opposed to distortion being a localized event in space. When computing indicators of non-linearity at one single position, one cannot infer that the measured distortion is a sign of presence of either cumulative or local distortion, as cumulative distortion is defined as being sustainable and being progressively built through space rather than just a brutal localized deformation of the waveform. Several example of cumulative distortion are wave steepening, shock formation and eventually shock coalescence. The first two are going to deform the waveform toward a saw-tooth wave and are therefore going to induce a shift in energy from the mid frequencies toward the high frequencies. On the other hand shock coalescence (due to the higher speed of stronger shocks) is going to reduce the number of zero-crossing and will results in a shift of the energy from the mid-frequencies toward the low-frequencies. As a global result non-linear distortion is going to broaden the overall spectra through space, helped by dissipation. The present study relies on the computation of both spectral and scalar indicators of non-linearity distortion to investigate its importance over the waveform while it propagates away from the jet.

II. The experimental set-up

A. The facility

The experimental campaign was conducted in Austin at the J.J.Pickle Research Center in the fully anechoic chamber in the Aerospace Engineering and Engineering Mechanics facility over a period of two days during Fall 2013 (25th and 26th of September). The anechoic chamber has its wall covered of melamine wedges and has the following internal dimensions from wedge-tip to wedge-tip : 18ft x 14ft x 12 ft. The cut-off frequency of the chamber is 100Hz and the normal incidence sound absorption percentage is 99%. The chamber possesses one upstream aperture that allows the entrance of entrained air due to the jet flow, and a downstream exhaust of dimension 6ft x 6ft acoustically treated that prevent any flow-blockage phenomena; this exhaust is then connected to an exit fan that eases the outflow to circulate. The nozzle exit, the inlet and the outlet are aligned on the jet center-line. The nozzle used has a geometry defined by the method of characteristics (MOC), and an exit diameter $D_j = 1in$ with a distance from the exit to the throat of 2.30in.

A more thorough description of this facility can be found in Donald *et al.* (2012)[4] and in Baars & Tinney (2013)[2] .

B. The experimental conditions

The campaign consisted in five testing sessions of approximately 2 hours each during which the atmospheric conditions were found to be fairly constant as it can be seen in table 1. The first 3 sessions were held the 25th at 5pm, 8pm and 11h30pm respectively; the last 2 sessions were held the 25th at 8pm and 10pm. All tests were run at fully-expanded conditions at a designed Mach number of 3.0 corresponding to a nozzle pressure ratio of 36.7. We compute the jet flow conditions using the classical quasi 1-D isentropic relations, assuming a ratio of specific heat of $\gamma = 1.4$ and a specific gas constant of air of $R = 287.05 J/Kg/K$. We then also define a common set of values chosen to minimize the differential error with all the tests; this error was found to be within 1.5% from all the jet flow characteristic values computed for all tests, and we therefore decided to use them for the rest of the study. These chosen values are also presented in table 1 in the last column. The interested reader is encouraged to refer to the paper of Baars & Tinney[1] to compare the experimental conditions of both test, that are found very similar and are not copied here for the sake of conciseness.
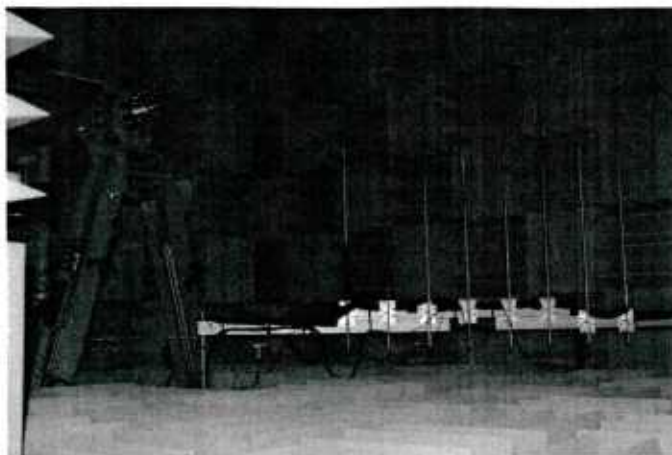
Figure 1. Overview of the anechoic chamber and the experimental set-up.

Measured Values						
Session	1	2	3	4	5	Average
$P_\infty[HPa]$	999	1000	1000	1001	1002	1000
$P_0[HPa]$	36700	36700	36700	36700	36700	36700
$T_\infty[K]$	308	306	302	304	303	305
$T_0[K]$	398	301	301	298	304	301
$HR\%$	35	40	43	50	57	NA
Computed Values						
Session	1	2	3	4	5	Average
$T_j[K]$	106.4	107.5	107.5	106.4	108.6	107
$a_j[m/s]$	206.8	207.9	207.9	206.8	208.9	208
$U_j[m/s]$	620.5	623.6	623.6	620.5	626.7	623.5
$f_j[kHz]$	24.4	24.6	24.6	24.4	24.7	24.5
M_j	3.0	3.0	3.0	3.0	3.0	3.0
M_a	1.77	1.78	1.78	1.77	1.80	1.78

Table 1. Experimental jet flow conditions, measured and computed based on quasi 1-d isentropic compressible flow equations.

C. Instrumentation and microphones placement

In order to obtain a constant Mach number, a CompactRIO system operates the control valves upstream of the nozzle through the use of a proportional-integral-derivative controller (PID) that allows to minimize the error by adjusting the percentage of aperture of the tuning valve. The variability of the NPR over all the tests was found to be less than 1%; Figure 3a shows the evolution in time of the valves aperture percentage along with the NPR. This figure shows how we operated the valves to reach a steady NPR value of 36.7 : we first open the main valve to a value of 10%, and when the NPR gets high enough we open manually to 35% the tuning valve, and at $t = 20s$ we turn on the PID controller. Once a steady NPR is reached, we starts acquiring data.

The data acquisition system consists in eight microphones that were simultaneously used during the experi-

3 of 13

ment are G.R.A.S. 46DD 1/8th inch of diameter plugged on 1/4th preamplifier; there frequency range is from 6.5 Hz up to 140kHz (+/- 2dB) while their dynamic range goes from 46dB to 179dB. These microphones are powered by a Dytran Instruments Inc. 4121 power supply sending a current of 5mA. The signal acquired is then low-pass filtered by a Khron-Hite corp filter, model FLX-3007, applying a 4th order Butterworth used here in order to reduce any aliasing error. Eventually the signal is then acquired at a sampling frequency of 500kHz at a 16bit resolution (range of -5V to +5V) with a PXI-1042Q using two NI-6122 boards connected to NI-2709 modules. We aquired at a largely over-sampled rate for the sake of resolution, and therefore accuracy in resolving shock-structures, which is crucial for a non-linear acoustic study.

Several region of the flow were investigated with these microphones. Data was acquired along four different arrays positioned at key angles (35°, 45°, 52° and 65°) which importance was highlighted in several past studies [12] . The origin of these arrays is positioned on the centerline in the post-potential core region of the jet that was found to be the apparent main source of sound radiated to the far field according to these same studies. An illustration of the placement of these arrays is given in figure 2. Identifying the right propagation path is a sensitive problem in the current analysis, as the jet doesn't behave like a single compact source, especially when we get closer to its hydrodynamic part. Choosing the wrong path would artificially trigger the apparition of non-linear distortion in the signal and one might interpret this as the sign of the presence of wave steepening of other cumulative non-linear distortion, this problematic has been addressed in past studies[12] . It was pointed out above that it is of great interest to perform measurements as close as we can get to the source, without endangering the microphones, and they were therefore placed as following. From $\rho = 13D_j$ (distance along the array, not from the centerline) with a $10D_j$ increment for angles 65° and 52°. At 35° due to the growth rate of the jet and in order to keep a safe distance from the hydrodynamic fluctuation that might damage expensive instruments, the first microphone was placed at a distance of $43.5D_j$. 45° corresponds to the Mach angle and the previous experiment showed its particular relevance, and it was therefore decided to give it a particular attention with 2 sets of measurement : one on the "near-field", from $\rho = 13D_j$ with a $5D_j$ increment, and one on the "far-field" from $\rho = 35.35D_j$ with a $10D_j$ increment between the eight microphones. The microphones were all placed in the horizontal plane of the jet centerline, but then their height was slightly set in a crescent order to avoid the first microphone to obstruct the others (though the change in height remains negligible).

Figure 3b quickly jumps to some preliminary results of the experiment to present a check of the microphone placement. Assuming a sonic convective speed (i.e. being outside of the hydrodynamic part of the jet), the time-lag between each signal obtained through cross-correlation gives us another way to compute the real spacing between the microphones. These values are then compared to the experimental spacing and should therefore be as close as possible from the identity curve. The good results obtained through this check are encouraging and validate our experimental protocol. It can be observed that the further away, the bigger the error gets; this is due to the fact that the signal of reference for the cross-correlation was the first one on the array, and therefore the error in spacing increases progressively while we move further away from it.
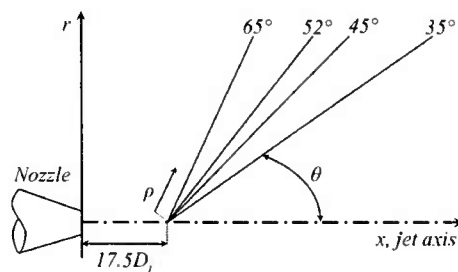

Figure 2. Illustration of the different microphones arrays set-up.

Several differences with the previous experiment of Baars & Tinney are relevant here. First of all the humidity rate has a known influence on the absorption coefficient of the medium through which the sound waves propagate.[3] This aspect will be further developed in the final paper but it might be possible that
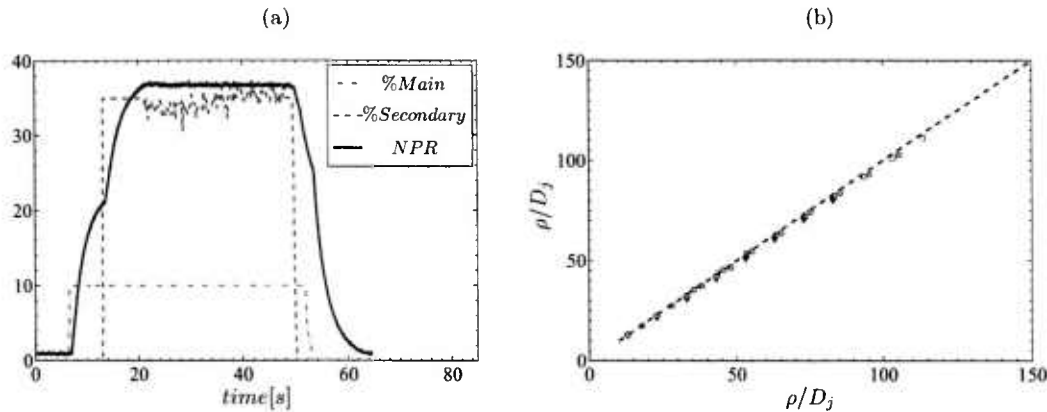
Figure 3. (a) NPR as a function of time for a typical data acquisition test and (b) Comparison between microphone placement and correlation assuming a sonic convective speed.

running at very high humidity rate actually increases the atmospheric absorption; this will consequently reduce the amplitude and the strength of the waveform, and prevent the waves to steepen enough to produce shocks. The impact of this last statement would dramatically changes the result of this present study. Then we must underline the quality of this new set of microphones that resolve frequencies up to 140kHz, while the previous microphones, 1/4th 46BD, have a range of resolution that stops at 70kHz. Finally, as pointed out in the introduction this experimental set-up takes into account the results of the previous experiment, and is therefore investigating for traces of cumulative non-linear distortion closer to the sound source, i.e. the jet.

III.   The jet acoustic

A.   Application of 2nd order high-pass filter

Before further analysis we apply a second order high-pass filter to the data in order to prevent the very-low frequency noise to influence the results, as illustrated in figure 4. The frequency cut-off of the anechoic chamber being at 100Hz, we start observing at low frequency some noise. The frequency cut-off of the filter was set at 300Hz, and is slightly adjusted for each microphone.

Figure 4. Illustration of the high-pass filtering on a typical spectra for one of the microphones.

B. Sound Pressure decay

As it is detailed below in the section IV. A, the computation of non-linear metrics are defined as being valid under the assumption of a spherical source ($1/\rho$ decay). It is therefore necessary to check if the decay does present a linear trend, indicating that we are indeed along the propagation path. Figures 5 and 6 are presenting the experimental results along with the analytically cylindrical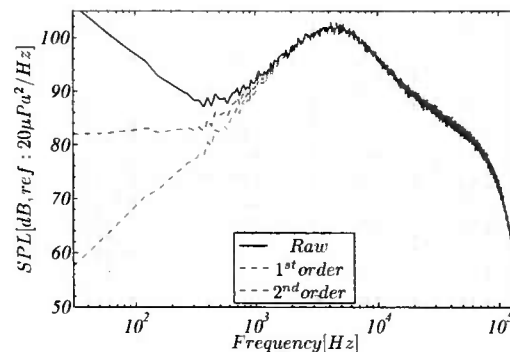 and spherical decays. It was shown through the application of wave-packet theory that the sound pressure decay is expected to follow a cylindrical law when close to the jet[7][12] (i.e. in $1/\sqrt{\rho}$ instead). The interest of using wave packets in modeling the generation and propagation of noise generated by large-scale turbulent structures in jet flows has been presented in several studies[5][7][12] . It can be observe indeed a good matching between the experimental decay and the spherical one when far enough from the jet for all angles. The plots for 35° and 52° (not presented here for the sake of conciseness) are similar to 45° and present also a good matching with the spherical decay law, although 45° is the angle where this trend hold closer to the jet. A matching with the cylindrical decay trend appears more clearly at 65° : figure 6b shows that the growth of P_{rms} possesses an inflection around $\rho = 50D_j$, which indicates that the array of microphone is close enough to the jet to capture the transition zone. This is in interesting finding as it means that this transition occurs far enough from the hydrodynamic region to be safely studied experimentally, and could be the focus of a future paper.

Further spectrum comparisons for different positions along the arrays and different angles will be shown in the final paper.

(a)   (b)
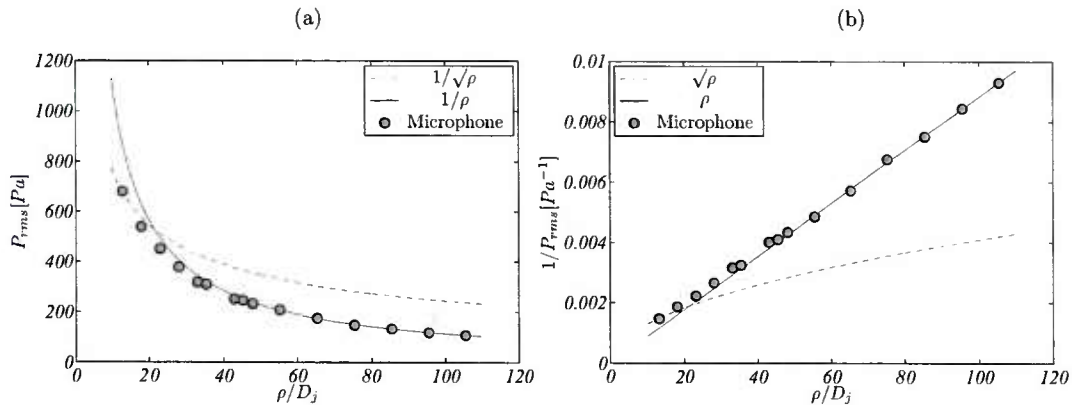
Figure 5. P_{rms} decay (a) and P_{rms}^{-1} growth (b) at 45d.

IV. Quantification of non-linearities

A. Spectral indicators

In this section we will present preliminary results regarding the quantification of non-linear distortions observed in the pressure field. This particular sub-section deals with spectral indicators (as opposed to scalar indicators that are not frequency-dependent).

The effect of cumulative non-linear distortion on the spectrum was described above, and several metrics based on spectral analysis have been developed in the past to quantify them. One of them is the Morfey-Howell indicator introduced in 1981[11] by Morfey & Howell. In the case of a spherical wave the modified Burger's equation can be modified in the following equation 1, where S_{xx} is the double-sided power spectral density, Q_{p^2p} the quadrature spectral density defined in equation 2 (where F is the Fourier transform), and the rest are constant values.

$$\frac{\partial}{\partial r}(r^2 e^{2\alpha r} S_{xx}(r, f)) = 2\pi f \frac{\beta}{\rho_\infty c_\infty^3} e^{2\alpha r} Q_{p^2p}, \tag{1}$$

6 of 13
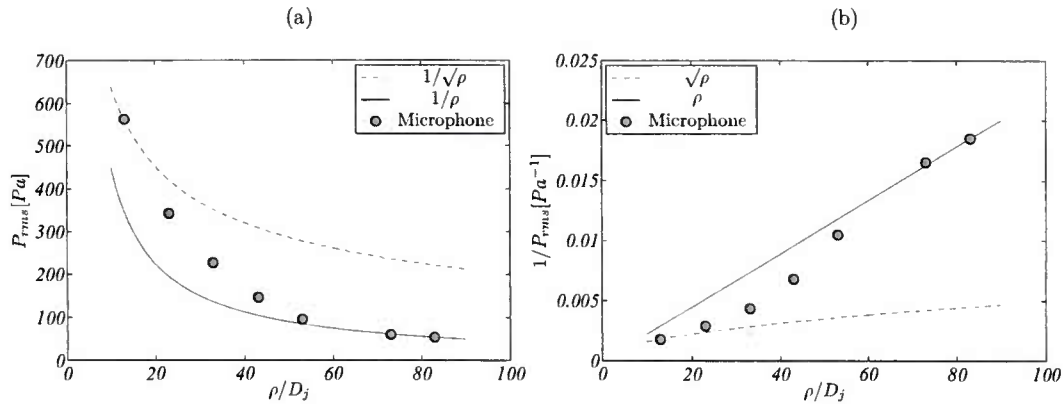
Figure 6. P_{rms} decay (a) and P_{rms}^{-1} growth (b) at 65d.

$$Q_{p^2p} = -Im(2F(p^2)F^*(p)), \tag{2}$$

In this equation Q_{p^2p} would equal zero according to linear theory, and therefore this term accounts for the nonlinear distortion of the spectrum assuming a spherical propagation, which is a limitation here as the jet acts as a non-compact source. However figure 5 illustrates how the spherical decay law stays valid over a broad range along the array positioned at $45°$ from the centerline. As underlined by Morfey & Howell it is more convenient to consider the normalized version of this indicator. Another indicator derived from the quadrature spectral density is Q_{p^2p}/S_{xx} giving a dimensionless quantity; both of them will be computed and are presented in equations 3 and 4.

$$Q = \frac{Q_{p^2p}}{P_{rms}^3}, \tag{3}$$

$$\frac{Q}{S} = \frac{Q_{p^2p}/P_{rms}^3}{S_{xx}/P_{rms}^2} \tag{4}$$

Figure 7a shows for the 4 different arrays the profiles of (filtered with a 1% moving bandwidth filter) for all the microphones. It is remarkable that these profiles end up collapsing, at least for the last 4 microphones of each array, i.e. for the last $40D_j$, which profiles are represented in red. These two indicators exhibit the same features of nonlinear distortion, and the same trend appears for the $\frac{Q}{S}$ in (b) although the profiles are a bit more noisy due to the normalization of Q by S_{xx}. It is important to note that for a truly Gaussian signal, i.e. without any nonlinearity, these indicators are flat over the entire spectra. As expected, Q/S is showing a lost of energy in the mid-range frequencies due to the nonlinearities present in the waveform, with a small increase in the low-frequencies due to shock coalescence (see figure 10a), and a strong increase in the high frequencies due to the abrupt shock structure. The fact that these spectrum eventually collapse means that no further nonlinearity distortion are added to the waveform. However the strong rate of change observed over the first microphones of the arrays are suggesting that measurable cumulative distortion is present. One array, the one located at a steep angle of $65°$ is however showing instead of a growth of nonlinear distortion a drastic decrease. This is consistent with past results[12] where it was observed that shock structures were concentrated mainly along the Mach angle ($45°$ for these jet conditions).

Figure 9 is showing the interpolated surface for all the microphones array of the evolution of the Morfey-Howell indicator, showing more clearly how the space can be divided in two areas. The first one where the spatial rate of change along the array is negative at $35°$, $45°$ and $52°$, which means that more and more distortion is added to the waveform, and then the second one where a steady state is reached and no more cumulative activity is measured. Once again, the array located at $65°$ is at the opposite showing a positive

rate of change in the first area, meaning that as the array of microphones leave the vicinity of the Mach angle, the waveform measured present less nonlinear distortion.

Finally, figure 8 shows the relatively low error induced by the bandwidth filter by comparing it with a typical raw spectra.

(a)   (b)
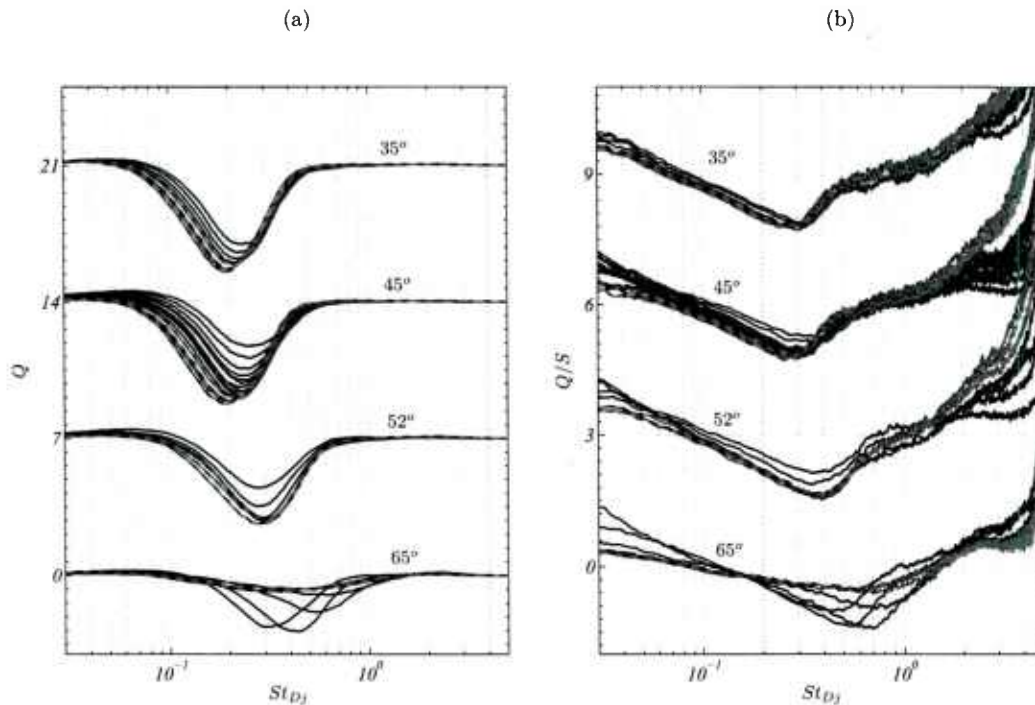
Figure 7. Raw (a) and normalized by the PSD (b) Morfey-Howell indicator (1% bandwidth moving filter) for all microphones (black) and for the last 4 microphones (red).

B. Scalar indicators

Scalar indicators are statistical metrics used to measure the impact of non-linear distortions over the pressure field along our four arrays of microphones. However they do not provide any information to differentiate local to cumulative distortion as they capture both of them.

The first one we will present is third moment of the time derivative of the pressure waveform, its skewness;this indicator is defined in equation 5 as being the mean of the $3^r d$ power of the time derivative of the pressure waveform, which is then normalized by the $3^r d$ power of the standard deviation of the time derivative of the pressure waveform. We focus our attention to the pressure derivative rather than its raw signal as it was shown by McInerny (1996)[9] how the statistics of gradients are much more sensitive to the presence of shocks.

$$S(\dot{p}) = \overline{\dot{p}^3}/\sigma^3 \tag{5}$$

As mentioned previously one of the consequences of cumulative non-linear distortion is the presence of shock coalescence, which footprint on the signal is a regular decrease in the number of zero-crossing throughout the waveform along the propagation path.

Figure 10 is presenting a comparison along the array at 45° for the different scalar indicators between the new experiment, the previous one, and the new one re-sampled at 100kHz which corresponds to the

8 of 13
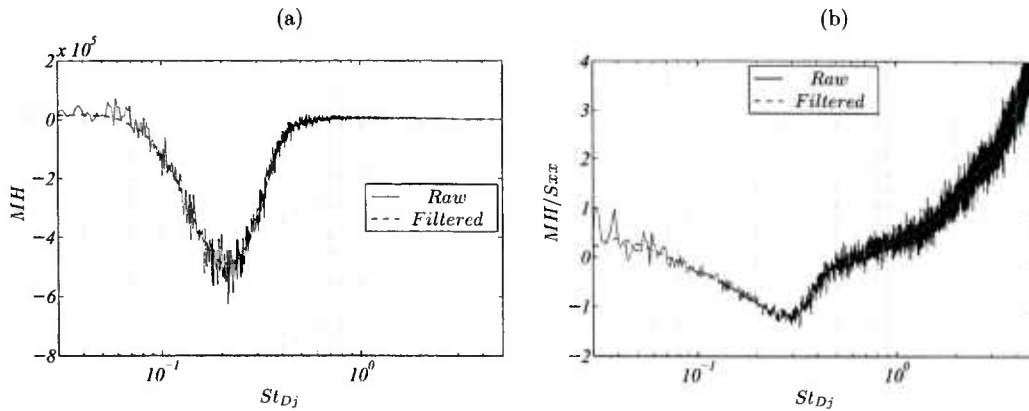
Figure 8. Comparison between the raw and smoothed data (1% bandwidth moving filter), typical plot.
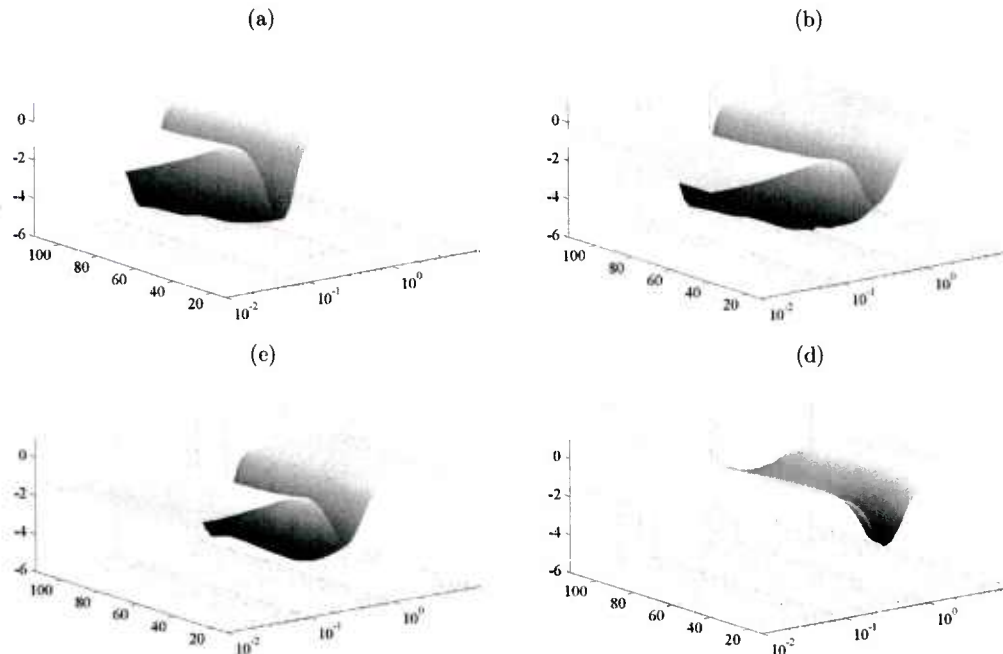
Figure 9. Evolution of the Morfey-Howell indicator along (a) 35° (b) 45° (c) 52° and (d) 65°.

sampling frequency of the previous experiment. Figure 10a is showing the evolution of the number of zero-crossing along the array of microphones and presents a clear decreasing trend. Surprisingly, this trend is not captured, or at least very attenuated, when the data is re-sampled to 100kHz. Besides, it seems that this trend eventually converges once far enough from the sound source. An approximation of the decay of N_{zc} is shown on the right in figure 10b, and its spatial derivative along the array of microphone is presenting a very singular shape, identifying three different zones. The first one, close to the source, where the rate of change

is constant; the second one where the decay of N_{zc} starts to evolve (the linear trend is due to the type of fitting chosen, but seems to match well with the data), and the third one where N_{zc} has converged. This is the typical footprint of a consistent shock coalescence along the microphone array, one type of cumulative non-linear distortion.

Now let's look at the evolution of $S(\dot{p})$ in figure 10c, there are several relevant feature to describe. First of all, three trends corresponding to each data-set (same legend as in figure 10a) are clearly present. The new data-set sampled at 500kHz shows a quasi-linear growth of $S(\dot{p})$ that can be attributed to a regular wave steepening as a skewness greater than 1 means that the probability density function is far from being a Gaussian and present strong asymmetries. After a certain distance along the array the steepening starts to reduce and ends up being approximately constant. Once more the previous experiment appears unable to capture the same trend and present a much more attenuated growth (but still observable), which is imputable to the differences between the experiments described at the end of section C. Finally the evolution of $S(\dot{p})$ for the re-sampled new data-set is noticeably intermediate : this shows how the sampling frequency by itself has a strong impact on the computation of non-linear metrics; besides we can deduce that the difference in amplitude between the two data-sets sampled at 100kHz is likely due to the other main different factor between the two experiment, which is humidity rate.

Finally, the last two figures (e) and (f) are presenting another scalar indicator which corresponds to the net flux of energy transfer across the Morfey-Howell spectrum shown is figure 7. By restricting the integration over only the negative part of the spectra which is localized in the middle of the range of resolved frequencies, we avoid the very low and frequency noise at the borders; besides it computes the flux of spectral energy being lost by the mid-range frequency due to cumulative distortion and is therefore a relevant indicator. Here we can observe once more a trend very similar to $S(\dot{p})$ with a remarkably linearly growth at the start of the array when being close the source. Further away the evolution starts to decrease and eventually as it the spatial derivative cancels.

Figure 11 shows on the same figure the evolution of the spatial rate-of-change along the array for these three indicators, each of them normalized in absolute value by by there maximum amplitude. This re-scaling is motivated by the fact that when looking for instance at the number of zero-crossing, a negative rate of change will indicate the presence of cumulative non-linear distortion. All these indicators are presenting a similar shape, which can be interpreted as an indication that strong cumulative non-linear distortion activity is concentrated in a region close to the source. It stays constant at the beginning of the array, showing that the spatial positioning of the microphones was close enough to the jet to capture the activity near the source : we can assume that getting closer to the source wouldn't provide much more information as a steady state seems to be reached. Then as the indicators start to decay, we can interpret this as the fact that the wave steepening as fully developed the waveform in a saw-tooth wave, which means that no further steepening can occurs. A direct comparison of the raw acoustic waveform in presented in subsection C will serve as a check and an illustration of these interpretations.

The final paper will encompass the same analysis for all the different arrays, in order to investigate for some directivity pattern in the wave steepening activity. Furthermore, overlaying the spectra of all microphones at different locations, once corrected for the dispersion and atmospheric absorption, should provide an interesting view of the frequency roll-off from the mid-frequencies to the higher (due to wave steepening) and lower (due to shock coalescence) frequencies.

C. Direct observation

Figure 12 presents a direct comparison of the raw pressure fluctuations along the 45° array. By using time-correlation we are able to track and superimpose the two correlated signals. Here we first compare the signals of two microphones located in the distortion zone which spacing is $30\ D_j$. This time-window was picked randomly and show a typical comparison between the two microphone signals. It appears that cumulative non-linear distortion effects described in section II. C can be observed in the form of wave steepening and shock coalescence at several locations in Figure 12a. At times 0.18, 0.55 and 0.64ms for instance the wave is noticeably more steepened for the signal at $\rho = 48D_j$ than at $\rho = 18D_j$. Besides it can be observed that the number of zero-crossing and high-frequency oscillations has been reduced when looking at portions of the signals comprised between 0.5 and 0.1, 0.2 and 0.3, and finally between 0.35 and 0.45ms, which is an indicator of shock coalescence. On the other hand the comparison between the two signals in Figure 12b doesn't present any feature that would suggest the presence of further cumulative non-linear distortion between the two microphone positions. We do observe that the shocks (in the form of N-waves, or saw-tooth
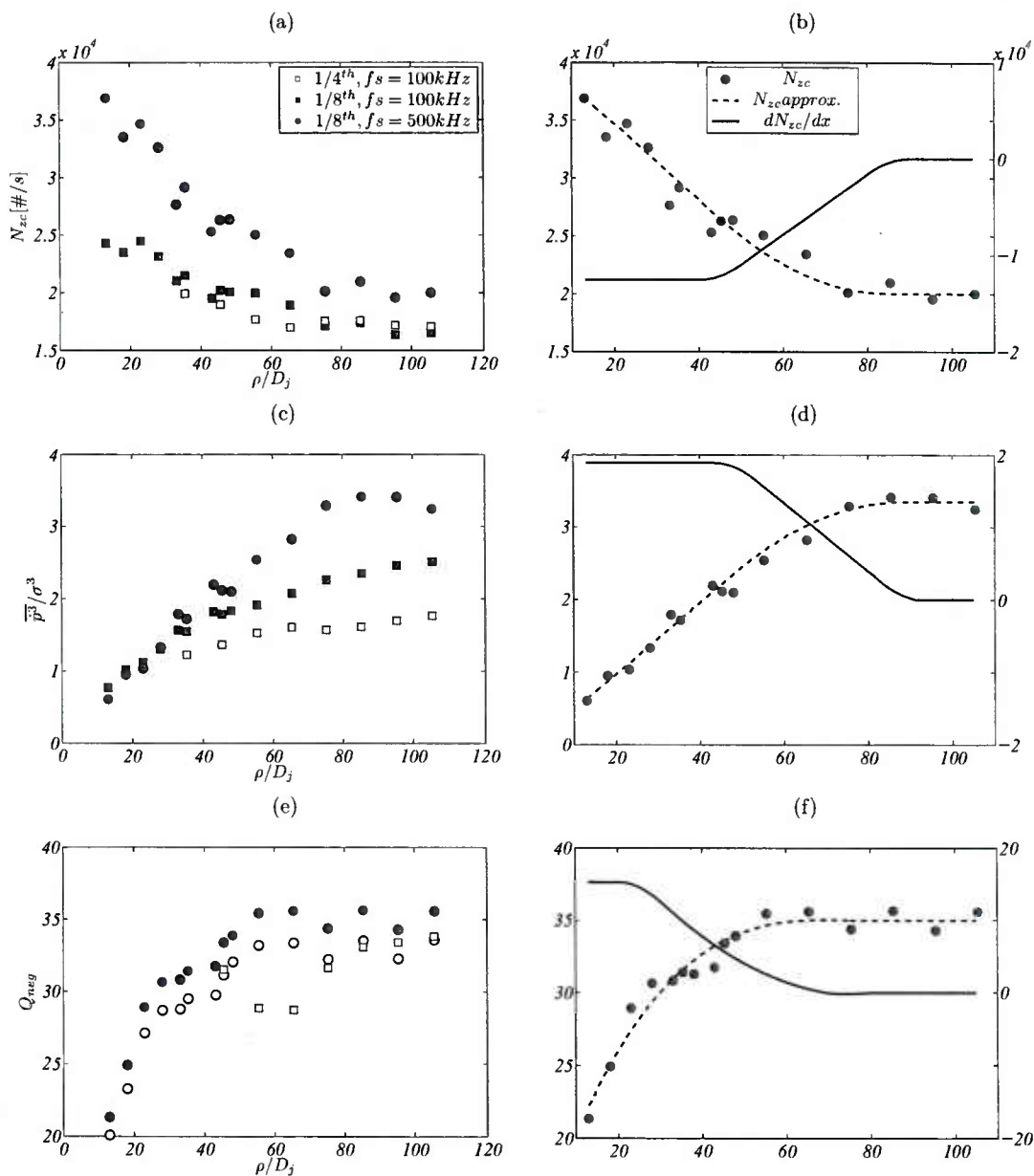
Figure 10. Number of zero-crossing N_{zc} (a), $\frac{\partial N_{zc}}{\partial x}$ (b), skewness of $\dot{p}$ (c), $\frac{\partial S(\dot{p})}{\partial x}$ (d), $-100Q_{neg}$ (e) and $-100\frac{\partial Q_{neg}}{\partial x}$ (f) for 45°.

waves) are already fully developed, at $\rho = 75D_j$, and that they are present at the exact same location at $\rho = 105D_j$. We reached "full saw-tooth shape" and therefore no further wave steepening can happen in this waveform which is going to decay in amplitude[8] .

11 of 13
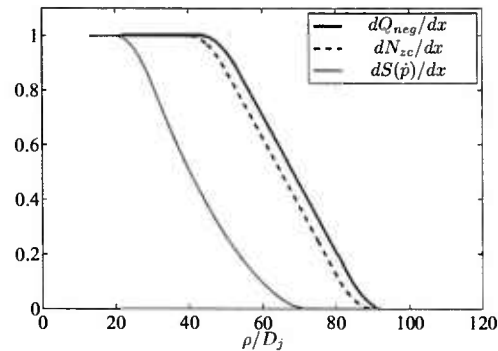
Figure 11. Comparison of the spatial derivative of the N_{zc}, $S(\dot{p})$ and Q_{neg} properly normalized in magnitude.

These observations are concordant with the results of the previous section where we observed that the non-linear distortion activity seems to be confined in the vicinity of the jet.
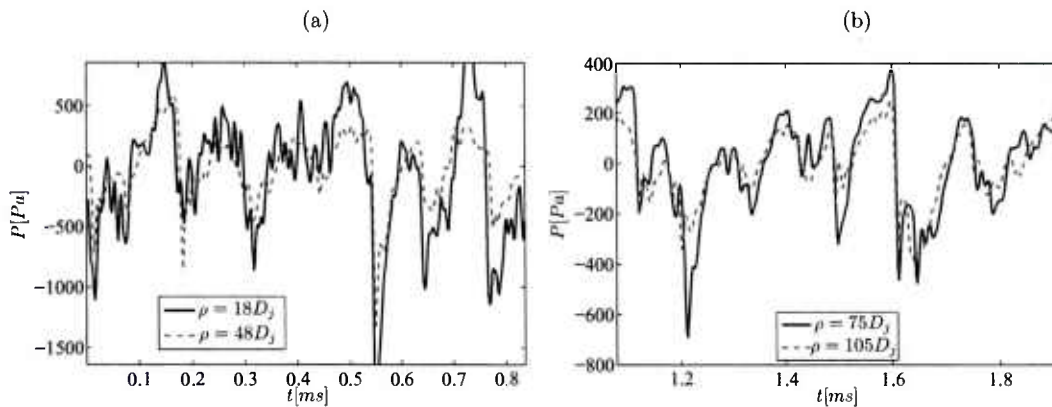
Figure 12. Evolution of the correlated pressure fluctuations between different position along $45°$ in the inner zone where wave steepening is present (a) and on the outer zone where it is absent (b).

V.   Acknowledgments

References

[1]BAARS, W. J., TINNEY, C. E. & WOCHNER, M.S., Nonlinear Propagation of Sound from a Fully Expanded Mach 3 Jet. AIAA Paper 2012-1177, 2012.

[2]BAARS, W. J., "Acoustics from high-speed jets with crackle" PhD thesis, The University of Texas at Austin, May 2013.

[3]BLACKSTOCK, D.T., Fundamentals of physical acoustics. John Wiley & Sons, Inc, New York, NY, 2000.

[4]DONALD, B.W., BAARS, W. J., TINNEY, C. E. & RUF, J.H., Acoustic characterization of sub-scale rocket nozzles. AIAA Paper 2012-0544, 2012.

[5]JORDAN, P. & COLONIUS, T., Wave packets and turbulent jet noise. Annu. Rev. Fluid Mech., Vol.45, pp.173-195, 2013.

[6]KROTHAPALLI, A., ARAKERI, V., Mach wave radiation : a review and an extension. AIAA Paper 2003-12000, 2003.

[7]KUO, C., DU, Y., McLAUGHLIN, D.K. & MORRIS, P.J., Experimental and computational study of near field /far field correlations in supersonic jet noise. AIAA Paper 2012-1170, 2012.

[8]HAMILTON, M.F. & BLACKSTOCK, D.T., Nonlinear Acoustics. Acoustical Society of America, 2008.

[9]McINERNY, S.A., "Launch vehicle acoustics part 2 : statistics of the time domain data." *Journal Aircraft* Vol.33(3), pp.512-523, 1996.

[10]McLAUGHLIN, S.A., "Experiments of the instability waves in supersonic jet and their acoustic radiation." *Journal of Fluid Mechanics* Vol.69(1), pp.73-95, 1975.

[11]MORFEY, C.L. & HOWELL, G.P., "Nonlinear propagation of aircraft noise in the atmosphere." *AIAA Journal* Vol.19(8), pp.986-992, 1981.

[12]PAPAMOUSCHOU, D., Wavepacket modeling of the jet noise source. AIAA Paper 2011-2835, 2011.

[13]TAM, C. K. W. & HU, F.Q., "On the Three Families of Instability Waves of High-speed Jets" *Journal of Fluid Mechanics* Vol.201, pp.447-483, 1989.

[14]TAM, C. K. W., "Mach wave radiation from high-speed jets" *AIAA Journal* Vol.47(10), pp.2440-2448, 2009.

APPENDIX A – PAGE A-14

QUARTERLY PROGRESS REPORT NO. 9 – N00014-11-1-0752

Approved for Public Release – Distribution is Unlimited

Appendix B: 2013 APS-DFD Abstract and Presentation, D24.00007
High Fidelity Measurements in the Far-Field of a Mach 3 Jet
Fiévet, Baars, Silva & Tinney

Abstract Submitted
for the DFD13 Meeting of
The American Physical Society

High fidelity measurements in the far-field of a Mach 3 jet RO-
MAIN FIÉVET[1], The University of Texas at Austin, WOUTIJN J. BAARS[2], The
University of Melbourne, DAVID SILVA[3], CHARLES E. TINNEY[4], The University
of Texas at Austin — Recent studies by Baars & Tinney (2012) [APS DFD12-
2012-002085] used 1/4inch pressure-field microphones to produce spatial mappings
of the far field spectra, OASPL, skewness and kurtosis of the pressure and pressure
derivative, as well as other indicators of local and cumulative nonlinear waveform
distortion (quadrature spectral density) of the sound field produced by a laboratory-
scale Mach 3 jet flow. It was shown that, despite the presence of crackle, cumulative
nonlinear distortions were absent along the peak noise path, where such effects have
been shown to reside in full-scale studies. The findings were supported by estimates
of the Gol'dberg number using relevant jet operating conditions. The experiment
of Baars & Tinney is revisited here using higher fidelity instruments (1/8th inch
pressure field microphones resolving up to 140kHz +/-1dB) to identify the effects
imposed by the larger microphones used by Baars & Tinney (2012).

[1]PhD Student
[2]Post Doctoral Research Fellow
[3]Undergraduate Student
[4]Assistant Professor

Romain Fievet
The University of Texas at Austin

Date submitted: 02 Aug 2013

Electronic form version 1.4

High fidelity measurements in the far-field of a cold Mach 3 jet

Romain Fiévet & Charles E. Tinney

Department of Aerospace Engineering and Engineering Mechanics,
The University of Texas at Austin, Austin, TX, 78712, USA

Woutijn J. Baars

The University of Melbourne, Parkville, Victoria 3010, Australia

THE UNIVERSITY OF TEXAS AT AUSTIN
Cockrell School of Engineering

THE UNIVERSITY OF
MELBOURNE

Pittsburgh, November 24th, 2013, Session D24, Acoustics II   66th Annual Meeting of the APS Division of Fluid Dynamics   fievetromain@utexas.edu

---

THE UNIVERSITY OF TEXAS AT AUSTIN
Cockrell School of Engineering

THE UNIVERSITY OF
MELBOURNE

The objectives

➤ Quantify the presence of **cumulative non-linear distortion (CNLD)** in the far-field of a Mach 3 fully-expanded cold jet

➤ Revisit the experiment of Baars & Tinney (2012)[1] with higher precision instruments

Baars & Tinney[1] experiment

- Four $1/4$th inch microphones, $f_s = 100$kHz, scanning the following Cartesian grid

- Provided topography of non-linear indicators, identifying directivity patterns

- Model based on a modified **Gold'berg #** predicting **shock formation distance = 18m** (Gaussian distribution at source)

→ *The shocks are created at the source or/and while undergoing strong CNLD in the close vicinity of the jet.*

OASPL mapping from Baars & Tinney (2012) [1]

[1] *Nonlinear Noise Propagation from a Fully Expanded Mach 3 Jet, Baars, W.J. & Tinney, C.E. AIAA 2012-1177*

Pittsburgh, November 24th, 2013, Session D24, Acoustics II   66th Annual Meeting of the APS Division of Fluid Dynamics   fievetromain@utexas.edu

THE UNIVERSITY OF TEXAS AT AUSTIN
Cockrell School of Engineering

THE UNIVERSITY OF MELBOURNE

The experimental set-up (1)

Instrumentation
- *GRAS:* Eight 46DD 1/8th in microphones
  - 6.5Hz to 140kHz (+/- 1dB)
  - 46 to 179dB
  - ~ 1mA/Pa
- $f_s = 500$kHz
- *Khron-Hite corp* FLX-3007 4th order Butterworth filter
- 16 bit resolution, range -5 to +5V

The facility
- MOC nozzle, $D_j = 1$ inch
- 99% normal incidence absorption above 100Hz
- Dimensions : 18ft x 14ft x 12ft

Jet operating conditions

			Measured Values			
Session	1	2	3	4	5	Average
$P_\infty[HPa]$	999	1000	1000	1001	1002	1000
P_0/P_∞			36.7 +/- 1%			36.7
$T_\infty[K]$	308	306	302	304	303	305
$T_0[K]$	298	301	301	298	304	301
$HR[\%]$	35	40	43	50	57	NA
			Computed Values			
Session	1	2	3	4	5	Average
$T_j[K]$	106.4	107.5	107.5	106.4	108.6	107
$a_j[m/s]$	206.8	207.9	207.9	206.8	208.9	208
$U_j[m/s]$	620.5	623.6	623.6	620.5	626.7	623.5
$f_j[kHz]$	24.4	24.6	24.6	24.4	24.7	24.5
$M_j = U_j/a_j$	3.0	3.0	3.0	3.0	3.0	3.0
$M_a = U_j/a_\infty$	1.77	1.78	1.78	1.77	1.80	1.78
$M_c = 0.8U_j/a_\infty$	1.41	1.42	1.43	1.42	1.44	1.42

Nozzle exit   *Array of microphones*

The anechoic chamber at the University of Texas at Austin (September 2013)

Pittsburgh, November 24th, 2013, Session D24, Acoustics II   66th Annual Meeting of the APS Division of Fluid Dynamics   fievetromain@utexas.edu

---

THE UNIVERSITY OF TEXAS AT AUSTIN
Cockrell School of Engineering

THE UNIVERSITY OF MELBOURNE

The experimental set-up (2)

Microphone placements
- **65° & 52°** : 13 to 83D_j ($\Delta\rho$=10D_j)
- **45°** : 13 to 48D_j ($\Delta\rho$=5D_j) & 35 to 105D_j ($\Delta\rho$=10D_j)
- **35°** : 43 to 113D_j ($\Delta\rho$=10D_j)

Experiment	Baars 2012	Fiévet 2013
$f_s[kHz]$	100	500
$f_c[kHz]$	50	140
Mic.placement	Grid	Arrays
$HR[\%]$	65 − 75	35 − 55

Differences between experiments

Microphone arrays

Cross-correlation along 45°:

Distance correlation vs. Microphone placement, assuming a sonic convective speed :

Pittsburgh, November 24th, 2013, Session D24, Acoustics II   66th Annual Meeting of the APS Division of Fluid Dynamics   fievetromain@utexas.edu

THE UNIVERSITY OF TEXAS AT AUSTIN
Cockrell School of Engineering

THE UNIVERSITY OF MELBOURNE

High-pass filter

- Apply a HP filter (f_c= 300Hz) to the data to suppress the low-frequency noise
- The metrics computed in the rest of the study are not affected by this filter

Arbitrary spectrum showing the influence of the HP filter

Pittsburgh, November 24th, 2013, Session D24, Acoustics II   66th Annual Meeting of the APS Division of Fluid Dynamics   fievetromain@utexas.edu

THE UNIVERSITY OF TEXAS AT AUSTIN
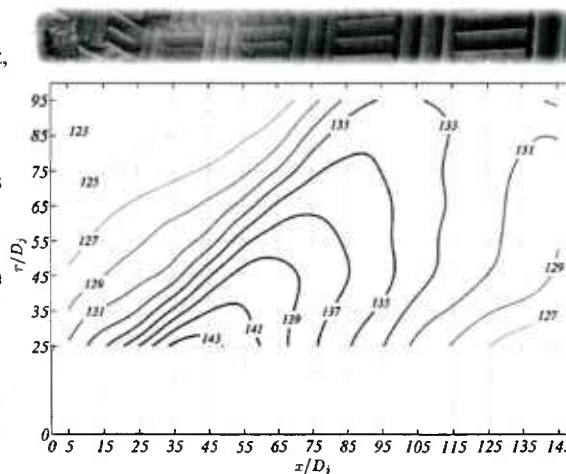Cockrell School of Engineering

THE UNIVERSITY OF MELBOURNE

P_{rms} decay

- Comparison to spherical/cylindrical[2] decay laws
- Verification of propagation path

[2] Kuo & al., "Experimental and computational study of near field /far field correlations in supersonic jet noise", AIAA Paper 2012-1170, 2012.

Pittsburgh, November 24th, 2013, Session D24, Acoustics II   66th Annual Meeting of the APS Division of Fluid Dynamics   fievetromain@utexas.edu

Slide 1

THE UNIVERSITY OF TEXAS AT AUSTIN
Cockrell School of Engineering

THE UNIVERSITY OF MELBOURNE

Spectral indicators

- The Morfey-Howell indicator[3]

$$\frac{\partial}{\partial r}\left(r^2 e^{2\alpha r} S_{xx}(r,f)\right) = 2\pi f \frac{\beta}{\rho_\infty c_\infty^3} e^{2\alpha r} Q_{p^2 p} \quad with \quad Q_{p^2 p} = -Im(2F(p^2)F^*(p))$$

$$Q = \frac{Q_{p^2 p}}{P_{rms}^3} \qquad \frac{Q}{S} = \frac{Q_{p^2 p}/P_{rms}^3}{S_{xx}/P_{rms}^2}$$

[3] Nonlinear propagation of aircraft noise in the atmosphere, Morfey, C.L. & Howell, G.P., AIAA Journal, Vol.19(8), pp.986-992 1981

Pittsburgh, November 24th, 2013, Session D24, Acoustics II   66th Annual Meeting of the APS Division of Fluid Dynamics   fievetromani@utexas.edu

Slide 2

THE UNIVERSITY OF TEXAS AT AUSTIN
Cockrell School of Engineering

THE UNIVERSITY OF MELBOURNE

Scalar indicators (1)

- These indicators quantify **locally** the distortion of the waveform.
- Their spatial rate of change gives information regarding **cumulative** distortion.

Number of zero-crossing → shock coalescence

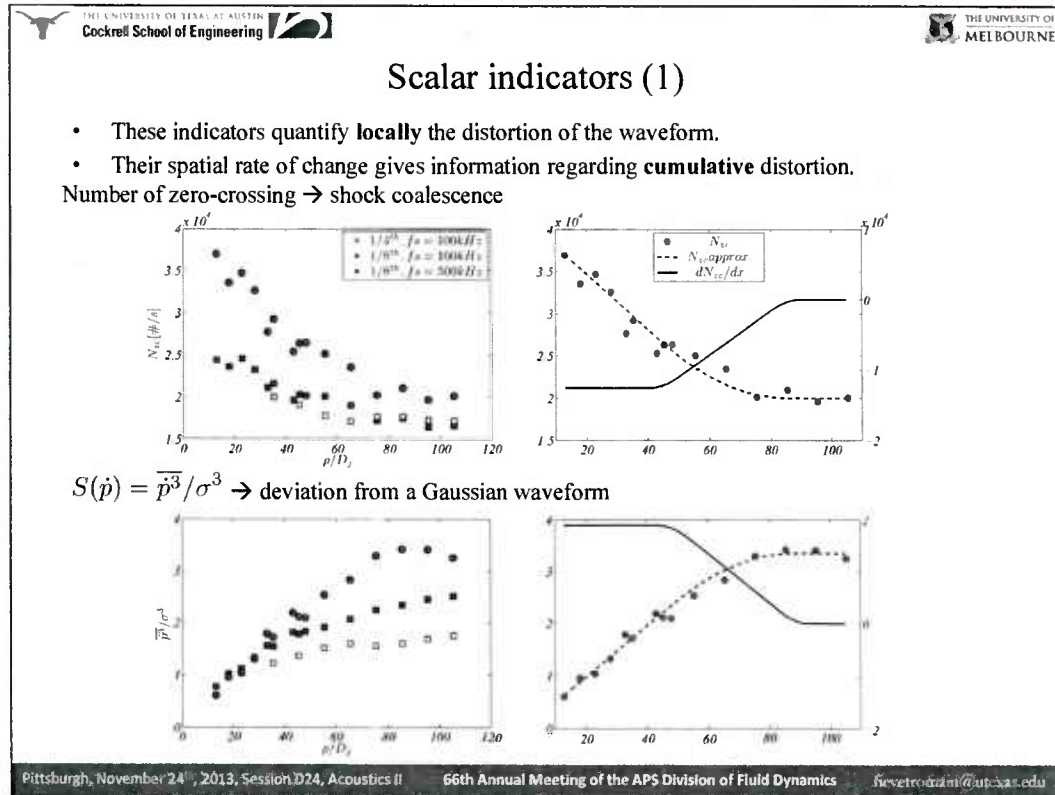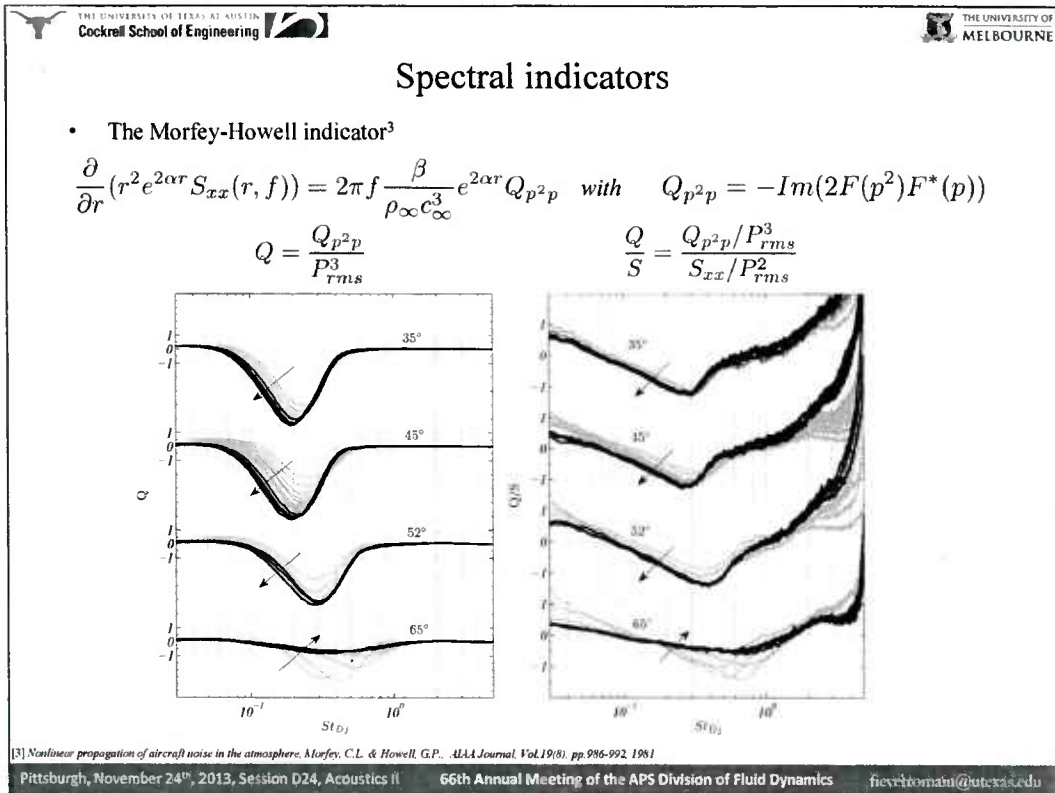$$S(\dot{p}) = \overline{\dot{p}^3}/\sigma^3 \rightarrow \text{ deviation from a Gaussian waveform}$$

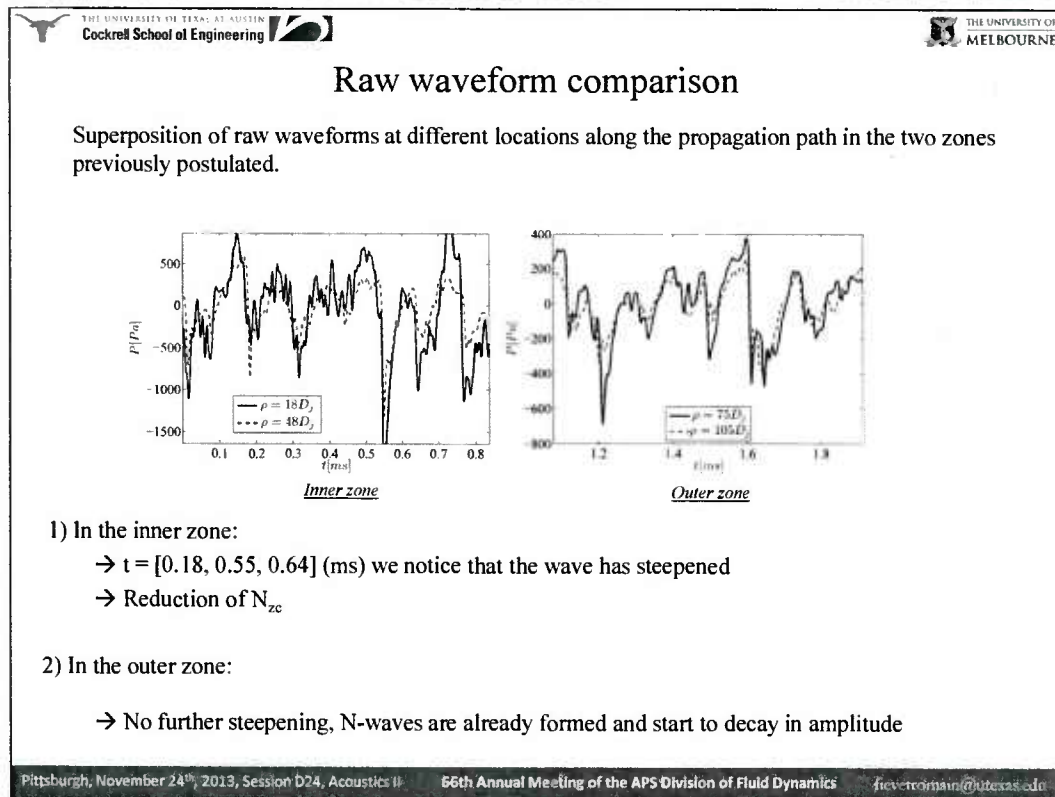

Pittsburgh, November 24th, 2013, Session D24, Acoustics II   66th Annual Meeting of the APS Division of Fluid Dynamics   fievetromani@utexas.edu

Scalar indicators (2)

$Q_{neg} = \int_{Q<0} Q(f)\, df$ → Flux of energy transfer in the Morfey-Howell spectrum

Observations
- Influence of f_s
- Potential CNLD activity close to the source
- Reach a steady state in the far-field
   - → 2 zones identified
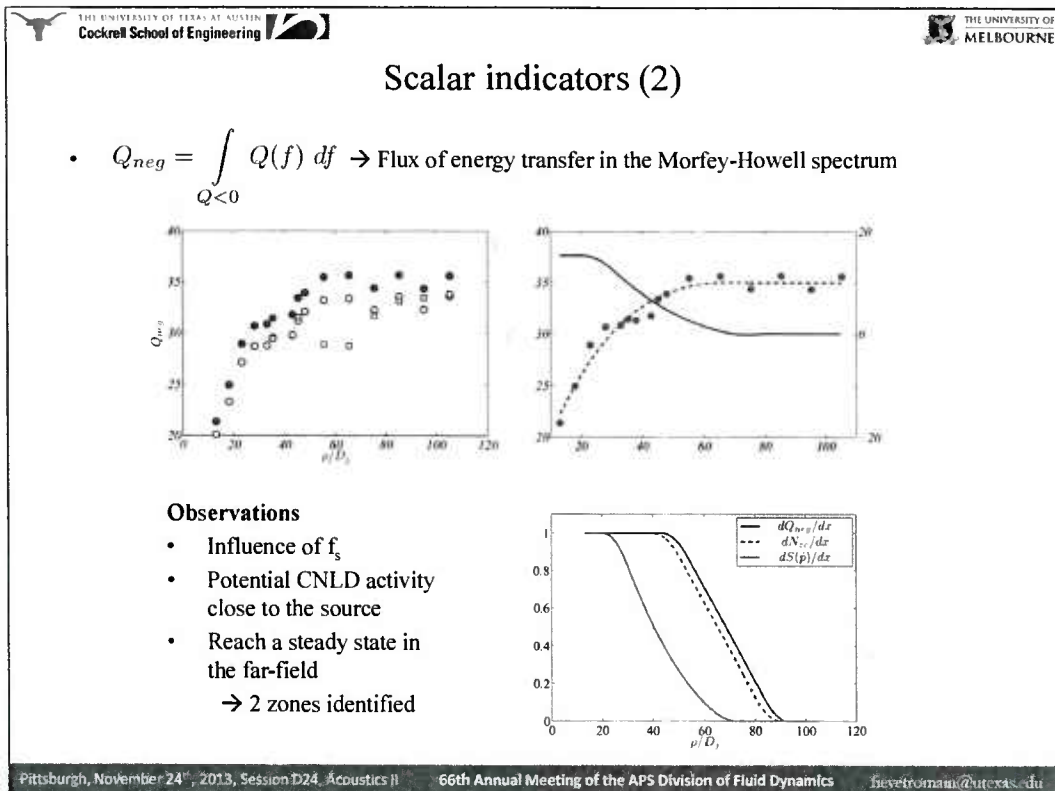
Pittsburgh, November 24th, 2013, Session D24, Acoustics II   66th Annual Meeting of the APS Division of Fluid Dynamics   fievetromain@utexas.edu

Raw waveform comparison

Superposition of raw waveforms at different locations along the propagation path in the two zones previously postulated.

Inner zone   *Outer zone*

1) In the inner zone:
   → t = [0.18, 0.55, 0.64] (ms) we notice that the wave has steepened
   → Reduction of N_{zc}

2) In the outer zone:
   → No further steepening, N-waves are already formed and start to decay in amplitude

Pittsburgh, November 24th, 2013, Session D24, Acoustics II   66th Annual Meeting of the APS Division of Fluid Dynamics   fievetromain@utexas.edu

THE UNIVERSITY OF TEXAS AT AUSTIN
Cockrell School of Engineering

THE UNIVERSITY OF
MELBOURNE

Conclusions

- CNLD activity in close vicinity to the jet
- No consequent distortion found on the far-field at this laboratory scale

Future work

- New experiment with only one microphone
  - → avoid discrepancies in the high frequencies to be detected as artificial CNLD
- Go closer to the jet (**outside of the hydrodynamic region**)
  - → capture transition between cylindrical/spherical decay
- Finer grid
  - → identify propagation path with greater accuracy

NPR = 36.7   NPR = 32

Pittsburgh, November 24th, 2013, Session D24, Acoustics II   66th Annual Meeting of the APS Division of Fluid Dynamics   favem.ronans@utexas.edu